Electrochimica Acta 326 (2019) 135005

Contents lists available at ScienceDirect

Electrochimica Acta

journal homepage: www.elsevier.com/locate/electacta

Two-dimensional anisotropic electrochemical behavior of carbon fiber

Chi Zhang [a], Xiaodong Chen [a], Guang-Ling Song [a, b, c, *], Dajiang Zheng [a], Zhenliang Feng [a], Yang Guo [d], Xiaosong Huang [e]

[a] Center for Marine Materials Corrosion and Protection, College of Materials, Xiamen University, 422nd. Siming Rd, Xiamen, Fujian, 361005, China
[b] State Key Laboratory of Physical Chemistry of Solid Surfaces, Department of Chemistry, College of Chemistry and Chemical Engineering, Xiamen University, 422nd. Siming Rd, Xiamen, Fujian, 361005, China
[c] School of Mechanical and Mining Engineering, The University of Queensland, Brisbane, Queensland, 4072, Australia
[d] Advanced Materials, China Science Lab, GM Global R&D, 56th. Jinwan Rd, Pudong, Shanghai, 200120, China
[e] Chemical and Materials Systems Lab, GM Global R&D, 30500 Mound Rd, Warren, MI, 48090, USA

ARTICLE INFO

Article history:
Received 5 September 2019
Received in revised form
2 October 2019
Accepted 3 October 2019
Available online 4 October 2019

Keywords:
Carbon fiber
Surface electrochemistry
Micro-electrode
Electrochemical sensor

ABSTRACT

The electrochemical behaviors of carbon fiber (CF) affect not only its mechanical properties in the aggressive environment but also the long-term durability of metals in contact. This study for the first time investigated the different electrochemical behaviors of the two-dimensional cross-section and cylindrical surfaces of a CF. Two specially designed carbon fiber electrodes (CFE) were used to understand the carbon fiber electrochemical performance in a 3.5 wt% NaCl solution. The results show that the CF is two-dimensional anisotropic in electrochemistry, and the cross-section is two orders of magnitude more active than the cylindrical surface. The strong polarization caused damage to the carbon fiber, particularly on the exposed cross-section.

1. Introduction

CF possesses high specific strength and modulus, good electrical conductivity and excellent resistance to corrosion [1–4]. There are mainly three types of CF based on precursors, polyacrylonitrile (PAN)-based, rayon-based, and pitch-based, among which PAN CFs dominate the current CF market [1,5]. When combined with various resin matrices, the formed CF composites offer unprecedented strength, modulus and weight advantages facilitating their use in different fields, such as sports [5], aerospace [6,7], automobile, etc. [8,9].

Nonetheless, bare CFs have poor adhesion to the matrices such as epoxy and nylon, because the carbonization of CFs at a high temperature could eliminate the polar elements in the original precursor materials [10], resulting in an inert surface. To improve the interaction between CFs and their matrices, functional groups have to be added to the surfaces of bare CFs via different approaches, such as chemical oxidation [11–15], electrochemical oxidation [16–20], and plasma treatment [21,22], in which, the electrochemical technique is the most effective and economic one. Various electrolytes have been used in the electrochemical oxidation, including ammonium salt [16,17,20,23], nitric acid [19], and potassium nitrate [24]. After the electrochemical treatment, the concentrations of oxygen and nitrogen functional groups on the CF surface markedly increase [18–20], and the chemical bonding between the CF and the matrices be effectively enhanced [10,18,23]. Also, the CF surface roughness can increase due to the etching effect of the oxidation treatment [10], which is favorable in increasing the adhesion strength physically. The surface treated CFs are then sized with a thin resin layer to improve the handleability before they are embedded into the matrix resin to make a composite.

Although many studies have been carried out on the electrochemical oxidation of CFs [4,10,17,25,26], most of the researchers focus their interests on improving the adhesion of CF with matrices [16,19,26,27]. Few papers have expressly investigated the electrochemical activity of the CFs, and the possible surface damage resulting from strong electrochemical reactions.

In this paper, the electrochemical behavior of a single CF was investigated with a focus on its electrochemical anisotropy.

* Corresponding author. Center for Marine Materials Corrosion and Protection, College of Materials, Xiamen University, 422nd. Siming Rd, Xiamen, Fujian, 361005, China.
E-mail addresses: glsong@xmu.edu.cn, guangling.song@hotmail.com (G.-L. Song).

https://doi.org/10.1016/j.electacta.2019.135005
0013-4686/

2. Materials and experimental

2.1. Material and solution

The CF bundles used in this study were the as-received PAN-based CFs (Panex 35 continuous tow, 50k) from the Toray Industries, Inc. (Tokyo, Japan). They were cleaned with copious deionized water and then with ethanol in a beaker under ultrasonication for 0.5 h, and then dried in an oven at 110 °C. The test solution used in this study was 3.5 wt% NaCl (equivalent to 0.6 mol/L NaCl, the NaCl concentration in seawater), which has been widely used to represent a typical corrosive environment in nature. It was selected in this study considering future applications of the CF in practice.

2.2. Specially designed single carbon fiber electrodes (CFEs)

Two single CFs selected from the cleaned CF bundles were packaged in two glass capillary tubes in two different ways, named as O-CFE and U-CFE, as shown in Fig. 1(a) and (b), respectively. It should be noted that both the O-CFE and U-CFE were made of a single carbon fiber (not a bundle of carbon fibers). In the O-CFE electrode, a straight single carbon fiber was inserted into a glass capillary tube, leaving the cross-section surface of the single carbon fiber exposed at the end of the capillary tube (i.e., the exposed cross-section surface of the single carbon fiber at the capillary tube end, looked like letter "O", would act as the working area of the electrode). In the U-CFE electrode, a single carbon fiber was bent into a shape of letter "U" and then inserted into a glass capillary tube, leaving the cylindrical surface of the bottom section of the "U" shaped single carbon fiber exposed out of the end of the capillary tube (i.e., the exposed cylindrical surface of the "U" shaped single carbon fiber out of the capillary tube end would act as the working area of the electrode). A Ni wire was connected to each of the CFEs through silver conducting paste in the capillary tube. After the paste was cured, both ends of the tube were sealed with epoxy resin to prevent possible ingress of water and other unknown substances into the tube. These two specially designed single CFEs guaranteed that the cross-section (see Fig. 1(c)) and the cylindrical surface (see Fig. 1(d)) of the CFEs would be exposed to the solution for measurements. The working surface areas of the O-CFE and U-CEF electrodes could be calculated from the diameter and the exposed longitudinal length of the CF.

2.3. Electrochemical measurements

Electrochemical measurements were carried out in a conventional three-electrode electrolytic cell, in which the working electrode (WE) was the CF, Ag/AgCl was the reference electrode (RE), and Pt foil was the counter electrode (CE), by using an electrochemical work station AUTOLAB (PGSTAT204).

The open circuit potential (OCP) was monitored in the test solution for each electrode before polarization. Potentiodynamic polarization was then conducted from −3 V to +3 V (vs. OCP) at a scan rate of 1 mV/s. A 2 h potentiostatic polarization was also performed at +3 V (vs. OCP) and −3 V (vs. OCP), respectively. Cyclic voltammetry was recorded at a scan rate of 10 mV/s between −3 V and +3 V (vs. OCP). In electrochemical impedance spectra (EIS) measurements, an AC potential amplitude of 10 mV was applied at the OCPs of the single CFEs in the frequency range from 10^5 Hz to 10^{-2} Hz, and 10 logarithmically spaced frequency points were collected per decade.

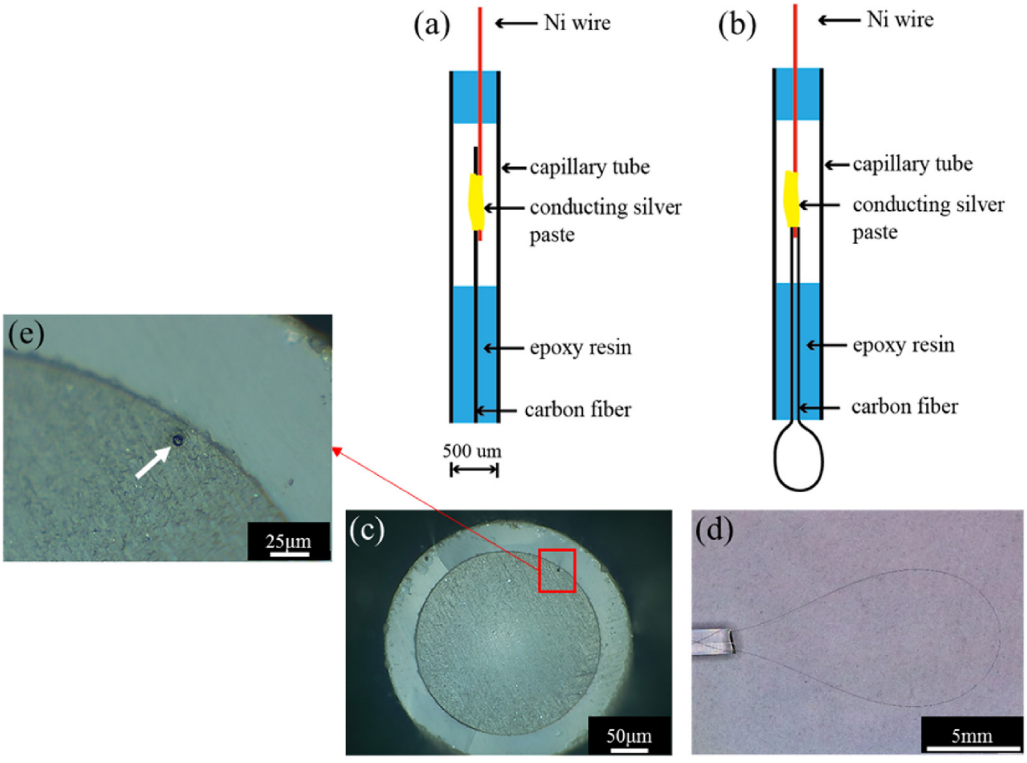

Fig. 1. Schematic illustration of the specially designed single CFEs. (a) O-CFE for cross-section and (b) U-CFE for cylindrical surface measurements, and the optical images of the actual CFEs: (c) the exposed cross-section of an O-CFE, (d) the exposed cylindrical surface of a U-CFE and (e) the enlarged area containing the exposed cross-section surface of the carbon fiber in the O-CFE.

2.4. Morphology characterizations

For an improved observation of the polarization effect on the possible damage of the CF, a CF bundle instead of a single filament was sealed in the glass capillary tube with epoxy resin as described above for preparation of the O-CFE and U-CFE, respectively. CFs were immersed in the test solution at the OCPs or different potentials for 2 h. After cleaning in water and drying, the surface morphologies of the CFEs were observed by a scanning electron microscope (SEM, TM3000 Hitachi, SU-70 Hitachi) at an accelerating voltage of 5 kV. The surface morphologies were further examined under an atomic force microscope (AFM, Dimension Icon Bruker) within a selected area of 3 μm × 3 μm.

3. Results

3.1. Electrochemical behavior

Fig. 2 shows the variation of the OCPs of the CFEs with time. The O-CFE reaches a relatively stable value at around −0.07 V right after its immersion in the 3.5 wt% NaCl solution, while the U-CFE becomes stable at around +0.20 V in 0.5 h. The O-CFE has a stable OCP about 250 mV more negative than the U-CFE.

The potentiodynamic polarization curves of the two CFEs are shown in Fig. 3. The OCP of the U-CFE is about 250 mV more positive than that of the O-CFE. The current densities of the O-CFE are always larger than those of the U-CFE in the whole potential range from −3 V to +3 V (vs. OCP), and the differences in polarization current densities between the U-CFE and O-CFE under the anodic polarization are larger than those under the cathodic condition. In addition, on the polarization curves of the O-CFE and U-CFE, there are two transition points where current densities increase suddenly. They are +1.8 V and −1.9 V vs. Ag/AgCl for the O-CFE and +1.7 V and −2 V vs. Ag/AgCl for the U-CFE. Moreover, platforms can be observed on the anodic polarization curves where the current densities are nearly constant with increasing potential in the range from +1.3 V to +1.8 V vs. Ag/AgCl for the O-CFE and in the range from +1.5 V to +1.7 V vs. Ag/AgCl for the U-CFE.

Cyclic voltammetric curves of the U-CFE and O-CFE are shown in Fig. 4. There are two peaks at +0.8 V and −0.9 V vs. Ag/AgCl for the O-CFE, and at +0.9 V and −0.8 V vs. Ag/AgCl for the U-CFE, which may correspond to two different redox reactions on the electrodes. The oxidation and reduction peaks on the O-CFE are much higher

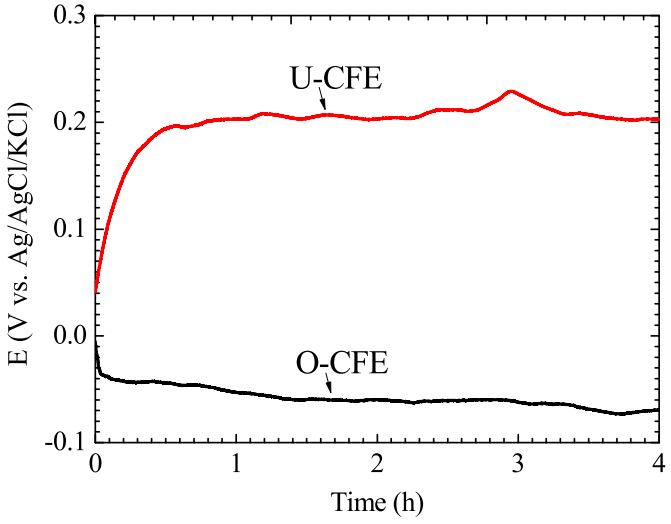

Fig. 2. Typical OCPs of the two CFEs immersed in 3.5 wt% NaCl.

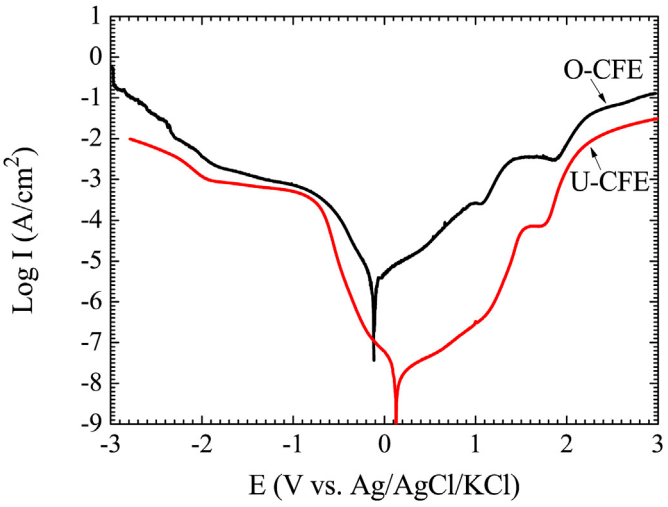

Fig. 3. Typical potentiodynamic polarization curves of the two CFEs in 3.5 wt% NaCl solution.

than those on the U-CFE; this could suggest that the O-CFE was much more electrochemically active than the U-CFE in the study.

The typical EIS results for the O-CFE and U-CFE at their OCPs are presented in Fig. 5. The EIS of the O-CFE is a semicircle on the Nyquist plot, while that of the U-CFE has a huge uncompleted loop, similar to a perfect organic coating before damage. The impedance of the O-CFE is much smaller than that of the U-CFE.

3.2. Surface morphology

The morphologies of the exposed cross-sectional and cylindrical surfaces of the CFs before and after the 2 h potentiostatic polarization treatments at different voltages are shown in Figs. 6 and 7. The original cross-section and cylindrical surface morphologies of the CFs can be seen in Figs. 6(a) and 7(a), respectively. In Fig. 6(a), the exposed round CFs (as pointed by the yellow arrows) have a diameter around 7 μm. There are tiny gaps between some of the CFs and the surrounding epoxy resin (as pointed by red arrows, see Fig. 6(a)). The cylindrical surfaces of the CFs appear to be covered by a thin polymer layer with a texture oriented in the longitudinal direction (see Fig. 7(a)). The SEM images of the cross-section and the cylindrical surface morphologies of the CFs after 2 h immersion at the OCPs are shown in Figs. 6(b) and 7(b), respectively. There are almost no changes on the morphologies of the CFs after immersion. After being polarized at +3 V for 2 h, obvious damages can be seen on both the cross-section and cylindrical surfaces (see Figs. 6(c) and 7(c)). The cross-sectional surfaces have been dissolved seriously, and some of the CFs have even disappeared from the monitored area (see Fig. 6(c)). “Groove” like damage areas can be observed on the cylindrical surfaces of the CFs (Fig. 7(c)), some of which are very deep. The exposed interiors of the CFs in the dissolved areas appears to be still linearly textured in the longitudinal direction, while the texture lines in the undamaged areas becomes insignificant. The damage is relatively mild under cathodic polarization. The O-CFE degradation is manifest predominantly as interfacial damage and CF erosion as indicated by the red arrows in Fig. 6(d). The cathodically polarized cylindrical surfaces become smoother, and the texture lines along the longitudinal axis are blurred (see Fig. 7(d)).

To avoid the possible decomposition of the substances formed on the CFs after the immersion and polarization treatments under high vacuum when being exposed to the SEM electron beam,

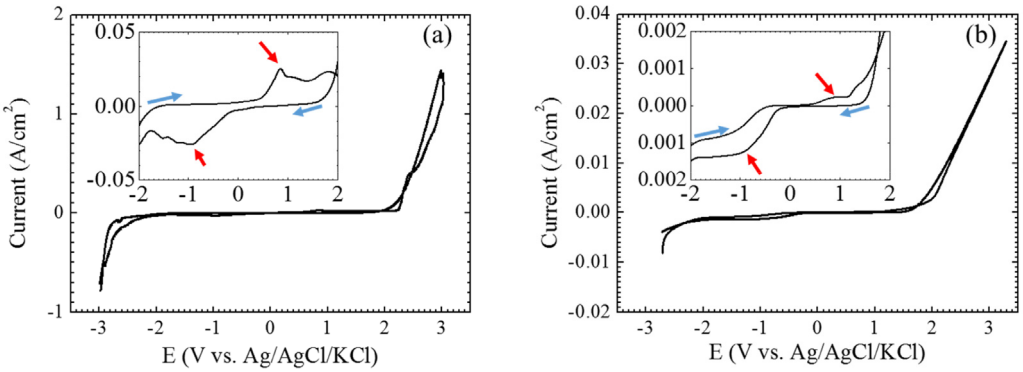

Fig. 4. Typical cyclic voltammograms of the two CFEs in 3.5 wt% NaCl: (a) O-CFE and (b) U-CFE.

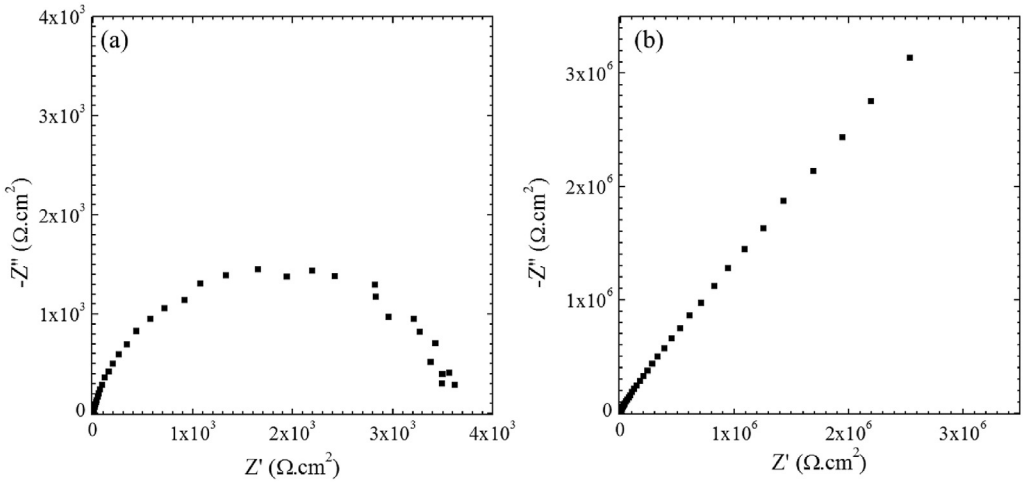

Fig. 5. Typical electrochemical impedance spectra of (a) the O-CFE and (b) U-CFE in the test solution.

leading to unexpected morphologic changes in the SEM chamber, the surfaces of the original and polarized CFs were further examined using an AFM, as shown in Fig. 8. The original texture lines on the surface can also be clearly seen (Fig. 8(a)). The round surface is flattened after anodic polarization (see Fig. 8(b)), confirming the dissolution of CF (see Fig. 7(c)). It is interesting that after surface dissolution, the exposed interior area of the CF treated under the anodic polarization condition still more or less keeps the linear texture (see Fig. 8(b)). These texture lines are probably inherited from the precursor PAN chains before carbonization. The AFM examination of the cathodically polarized CF surface (Fig. 8(c)) also further verifies that the original surface texture lines can become less evident after cathodic polarization (Fig. 7(d)).

4. Discussion

Carbon fiber is a fiber that contains over 90% carbon in a crystal structure similar to graphite, in which carbon atoms along the fiber longitudinal direction are connected by covalent bonds while the van der Waals force holds the bonded carbon atom layers (basal planes) together in the radial direction [28]. Particularly when the CF is made from a polymer, the long chain structure of the precursor can be inherited in the CF after carbonization to a great degree. This results in a structure where the chemically inert graphitic basal planes are aligned in the fiber direction, leading to a higher mechanical strength and lower electric resistance in the CF longitudinal direction than in its cross-section. Therefore, it is a straightforward inference that a CF with strong mechanical and physical anisotropies may also be electrochemically anisotropic, as the Femi energy level and the charge carrier density can differ in the longitudinal and radial directions of a CF due to the different lattice parameters on different surfaces.

The above postulation was experimentally verified in this study by the OCP, dynamic and potentiostatic polarizations, cyclic voltammetry and EIS measurements. All the results shown in Fig. 2~5 have indicated that the cross-sectional surface of a CF is electrochemically much more active than the cylindrical surface.

The OCP of the O-CFE reaches a constant voltage more quickly (see Fig. 2) than that of the U-CFE; this can be simply interpreted as the active cross-sectional surface has faster electrochemical reactions and thus can reach its steady state more quickly than the passive cylindrical surface. The OCP is more positive on the cylindrical surface (U-CFE) than on the exposed cross-section (O-CFE) (see Fig. 2), and that is because the alignment of the graphitic basal planes in the fiber direction and the CF surface treatment/passivation has more effectively inhibited the anodic processes than the cathodic reactions on the cylindrical surface (U-CFE).

In fact, pure carbon in theory is an electrochemically inert material, not participating in electrochemical reactions under a weakly polarized condition but providing a surface for the reactions to take

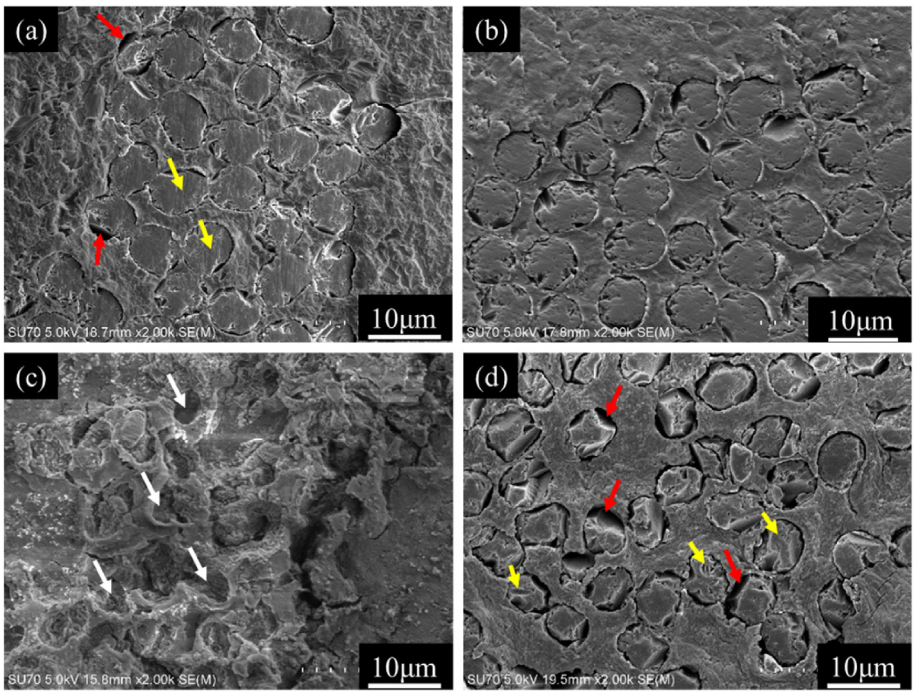

Fig. 6. SEM images of the cross-sections of CFs. (a) original cross-section surface, (b) cross-section surface after 2 h immersion at OCP, (c) anodically polarized cross-section surface at +3 V vs. Ag/AgCl for 2 h, (d) cathodically polarized cross-section surface at −3 V vs. Ag/AgCl for 2 h.

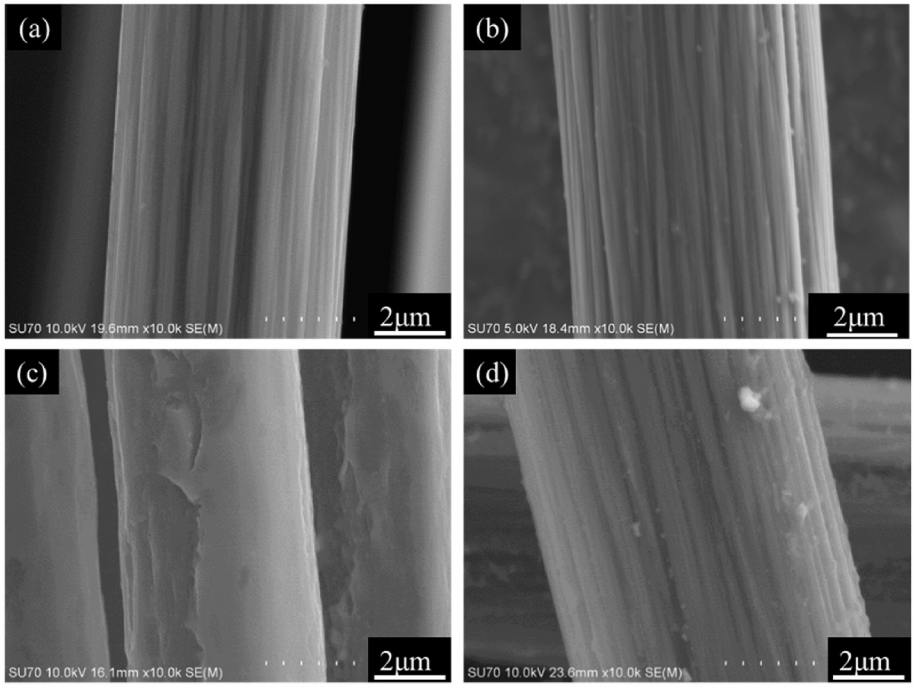

Fig. 7. SEM images of the cylindrical surfaces of CFs. (a) original cylindrical surface, (b) cylindrical surface after 2 h immersion at OCP, (c) anodically polarized cylindrical surface at +3 V vs. Ag/AgCl for 2 h, (d) cathodically polarized cylindrical surface at −3 V vs. Ag/AgCl for 2 h.

place in the test solution. However, CF is not pure carbon. It contains some impurities, such as H and some oxides of Si, K, Na, Fe, Mg, Ca from the precursor or the raw materials, as well as the manufacturing process, which may be dissolved/participate in reactions under certain strong anodic polarization conditions and its electrochemical activity may vary with potential [28]. In carbon fibers, the graphite basal planes are aligned in the fiber direction. The functional groups (impurities) are largely located at the basal plane edges. Therefore, the cross-section appears to be more active than the cylindrical surface, as the functional group content can be higher on the cross-section. In addition, the intercalation of molecules into the space between basal planes can also take place,

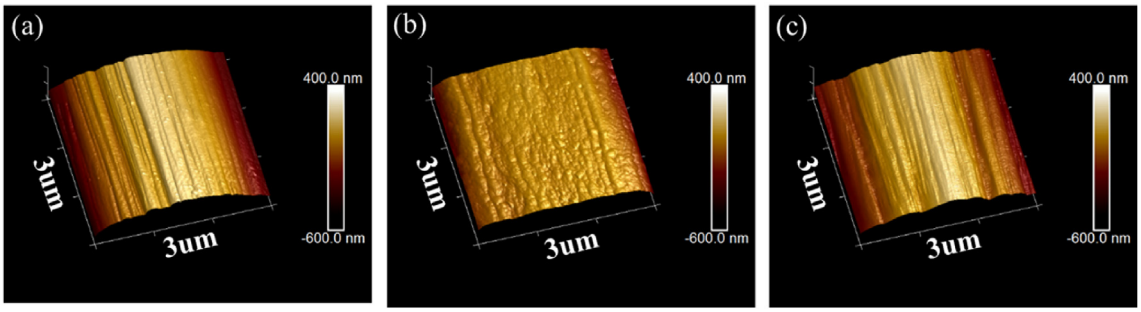

Fig. 8. AFM images of the cylindrical surface of a CF before and after 2 h of anodic and cathodic potentiostatic polarization at ±3 V vs. Ag/AgCl: (a) original surface, (b) anodically polarized surface, (c) cathodically polarized surface.

especially on the cross-section, which further increases its activity. The polarization curve measurements (see Fig. 3) show that, at around the OCPs, the decrease of the anodic polarization current densities from the cross-sectional surface to the cylindrical surface are more significant than the decrease of the cathodic polarization current densities.

On the measured polarization curves (see Fig. 3), from −0.3 V to +0.5 V vs. Ag/AgCl, the weakly polarized CF does not participate in an electrochemical process, but provides a surface for the electrochemical reactions. In this case, the main electrochemical reaction on a CF surface should be an oxygen redox process. Hence, the polarization curves have typical anodic and cathodic Tafel slope regions. On the cylindrical surface (U-CFE), due to the alignment of the graphitic basal planes and the presence of the passive surface layer, the anodic and cathodic polarization current densities are much smaller than those on the cross-section surface (O-CFE).

When the potential is more negative than −0.3 V vs. Ag/AgCl or more positive than +0.5 V vs. Ag/AgCl (see Fig. 3), the electrochemical processes should be mainly oxygen reduction and oxygen evolution, probably together with limited impurity dissolutions. The cross-section surface (O-CFE) is obviously more active for the oxygen redox reactions and the impurity dissolutions than the cylindrical surface (U-CFE).

On the cross-section surface (O-CFE), the increasing cathodic and anodic current densities reach their plateaus at around −0.8 V and +1.3 V vs. Ag/AgCl, respectively (see Fig. 3). It could be simply interpreted as that the cathodic reactions are limited by oxygen diffusion and the CF impurities have been significantly consumed or passivated, thus their respective contributions to the cathodic and anodic current densities become insignificant. On the cylindrical surface (U-CFE), the presence of the low activity basal planes and the passive surface layer can inhibit the oxygen reduction and evolution, probably as well as impurity dissolution. However, the surface layer might be damaged by cathodic polarization. Thus, the cathodic polarization current density at a potential more negative than −0.3 V vs, Ag/AgCl increases to a level close to that of the exposed cross-section (O-CFE). In the anodic polarization region, the anodic current density of the U-CFE continues increasing with potential and does not exhibit a significant plateau at around 1.3 V vs. Ag/AgCl. This can be because the impurity influence is limited under the anodic condition.

Under strong anodic polarization, an interesting observation of the polarization curves is the dramatic increase in current density at around +1.2 V ~ +1.5 V vs. Ag/AgCl followed by a current plateau and the other rapid current increase at around +1.8 V ~ +2.0 V vs. Ag/AgCl on both the cylindrical and cross-sectional surfaces (see Fig. 3). These sudden current increases have been observed on carbon fiber reinforced polymer composites (CFRP) in a previous study, in which they were marked as transition points caused by the breakdown of the matrices [29]. It is postulated here that the first anodic current rapid increase at around 1.2 V ~ +1.5 V vs. Ag/AgCl may correspond to oxygen evolution, which could further oxidize the CF surface, forming a new surface passive layer in the effective area, resulting in a current plateau at a higher current density. The second anodic current increase at around 1.8 V ~ +2.0 V vs. Ag/AgCl can be postulated to be associated with the breakdown of the newly formed passive layer, and consequently the CF can significantly dissolve. Both the anodic oxidation and anodic dissolution of the CF to some extent can destroy the cross-section and cylindrical surfaces.

Strong cathodic polarization can also lead to a current density increase at around −1.8 V vs. Ag/AgCl (see Fig. 3), which had also been detected and marked as transition points on the cathodic polarization curves of the CF in the previous study, attributed to cathodic hydrogen evolution [29]. The strong hydrogen evolution from the effective area of the cylindrical surface can cause debonding of the CF from the mounting epoxy resin (Fig. 6(d)), and an increase in exposed area of the cross-section surface (O-CFE). Hence, the cathodic current density on the cross-section surface (O-CFE) increases more rapidly than that on the cylindrical surface (U-CFE).

For the O-CFE, from the OCP to +1.2 V vs. Ag/AgCl (see Fig. 3), the polarization current densities of the O-CFE are about 3 orders of magnitude higher than those of the U-CFE, and their logarithmic polarization curves are almost parallel in this potential range. This means that the same anodic reactions occurred on these two different surfaces, but the total effective surface area for the reactions on the cylindrical surface is 3 orders of magnitude smaller than the cross-sectional surface. It is interesting that the difference in the anodic polarization curves of the O-CFE and U-CFE reduces to 2 orders of magnitude in the potential range from +1.2 V to +1.8 V vs. Ag/AgCl, and further down to less than 1 order of magnitude when the polarization potential is higher than +1.8 V vs. Ag/AgCl. These suggest that the total effective area for electrochemical reactions on the cylindrical surface increases with anodic polarization potential after +1.8 V vs. Ag/AgCl. In the cathodic direction, from the OCP of the O-CFE to −1.8 V vs. Ag/AgCl, the cathodic current density difference between the exposed cross-sectional surface (O-CFE) and the cylindrical surface (U-CFE) decreases from 2 orders of magnitude to about 0.2. After that, it increases again up to 1 order of magnitude at -3 V vs. Ag/AgCl. The difference between the cathodic polarization curves of the U-CFE and O-CFE does not significantly decreases with potential, implying that strong cathodic polarization cannot damage the passive surface layer/basal plane as seriously as anodic polarization. This is partially confirmed by the surface morphology observations (see Figs. 6 and 7), in which cathodic polarization cannot even evidently alter the linear texture on the cylindrical surface whereas anodic polarization can.

The electrochemical processes proposed above can be further

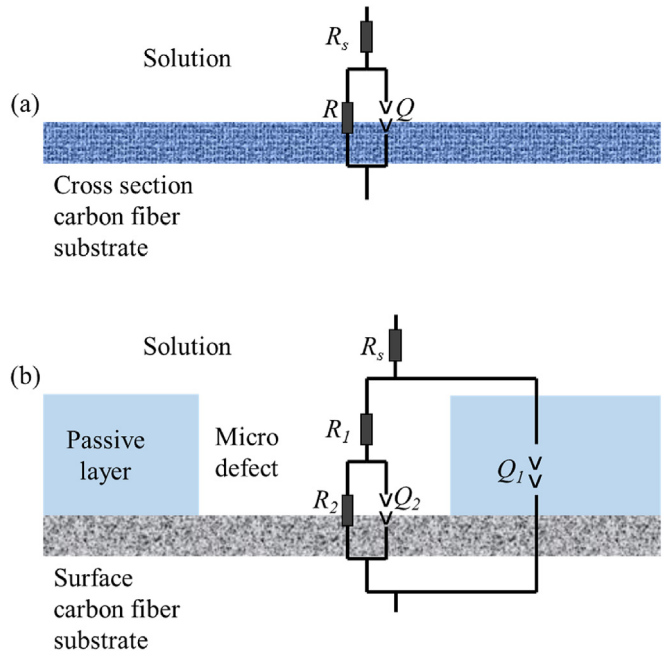

Fig. 9. Schematic illustration of the different surfaces of a CF and their corresponding equivalent circuits: (a) O-CFE (b) U-CFE.

supported by cyclic voltammetry. The oxidation and reduction peaks at around +0.8 V and −0.9 V vs. Ag/AgCl on the cylindrical surface (O-CFE) shown in Fig. 4(a) could be transient processes corresponding to the current density increases at +0.5 V and −0.3 V vs. Ag/AgCl on the polarization curve of the O-CFE (see Fig. 3), resulting from oxygen evolution ($4OH^- \rightarrow O_2 + 2H_2O + 4e^-$) and reduction ($O_2 + 2H_2O + 4e^- \rightarrow 4OH^-$) [30]. The much larger anodic and cathodic peaks at potentials more positive than +2 V and more negative than −1.8 V vs. Ag/AgCl (see Fig. 4(a)) should correspond to the dramatic current density increases at +1.8 V and −1.8 V vs. Ag/AgCl on the polarization curve of the O-CFE (see Fig. 3), caused by strong anodic dissolution of CF and cathodic hydrogen evolution ($2H_2O + 2e^- \rightarrow H_2 + 2OH^-$), respectively. Other small peaks in Fig. 4(a) represent more complicated electrochemical steps involved in the anodic and cathodic processes. The passive layer/basal plane on the cylindrical surface (U-CFE) may not be destroyed severely during a rapid voltammetrical scan as in potentiodynamic polarization. Hence, the above transient peaks are relatively low on the cylindrical surface (see Fig. 4(b)).

Based on the above analyses, a physical model for the electrochemical behavior of a CF is proposed here. The passive layer on the cylindrical surface is thin, containing some tiny defects, which are more electrochemically active than the other cylindrical surface areas, but less active than the cross-section surface. The CF consists of numerous organic molecular chains aligned in the longitudinal direction along the CF. Therefore, the cross-section and the cylindrical surface can be schematically illustrated in Fig. 9. Correspondingly, two different equivalent circuits as shown in Fig. 9(a) and (b) respectively can be employed to fit the measured electrochemical impedance spectra. The simple single-time constant equivalent circuit (see Fig. 9(a)) is proposed to simulate the electrochemical EIS behavior of the O-CFE, in which R and Q represent the resistance and the distributed capacitance of the exposed cross-sectional area and R_s is the solution resistance between the reference electrode and the exposed cross-sectional surface. Because of the presence of a discontinuous passive layer on the cylindrical surface of the U-CFE, a typical circuit normally used to represent a damaged coating (see Fig. 9(b)) is employed to simulate the EIS behavior of the U-CFE. In this two-time-constant equivalent circuit, R_1 is the resistance of the active defects in the passive layer, Q_1 is the capacitance of the passive layer containing these defects, R_2 is the resistance of the carbon substrate, Q_2 is the capacitance of the interface between the CF and the solution. With this model, the EIS results can be simulated and explained.

The estimated equivalent circuit elements are listed in Table 1, in which Q can be converted to C through the Brug approach [31]. The results show that the resistance R of the O-CFE is one order of magnitude smaller than R_2 of the U-CFE while the capacitance C of the O-CFE is one order of magnitude larger than C_2 of the U-CFE, indicating that O-CFE is much more electrochemically active than U-CFE. It should be noted that the capacitance C of O-CFE is around 20 μF/cm^2 (Table 1), which is a typical value of a double layer capacitance of a bare metal exposed to an aqueous solution [32–34], indicating the double layer formed between the bare CF surface and the solution is similar to that of a bare metal in solution. The differences of about one order of magnitude in capacitance and resistance of the CF on the cross-section and cylindrical surfaces imply that only about 10% of the apparent cylindrical surface is exposed to the solution through the defects in the passive layer. R_1 and C_1 (Table 1) of the passive layer have values of a nearly damaged coating system [35,36], suggesting that the passive layer on the cylindrical surface might be a porous film.

CF is generally believed to be a very stable material that can survive in various service environments. It has been recommended for some extreme applications [37–41]. However, the finding that strong polarization can cause serious damage on CF from this study may invert such an opinion. Hence, it will be important to decrease the electrochemical activity of CF with improved surface treatments and reduced surface defect numbers.

On the contrary, due to its high electrochemical activity and sensitive electrochemical response, the cross-section of a CF (O-CFE) can be developed into a micro electrochemical sensor or probe, which will have a high-resolution but with low cost and hence find many potential applications in practice. For example, if the CF bundles can be carefully placed in desired positions in CFRP, the CFRP may become a smart location sensor in some applications.

Another implication of the finding is that the cut edge of a CFRP sheet will be more active than the sheet surface. This is because the highly active cross-section surfaces of CF bundles are exposed on the cut edge, not on the sheet surface. Thus, the edge has a higher driving force to trigger the galvanic corrosion of the coupled metals [42]. How to prevent such an edge effect should be focused in the practical applications.

5. Conclusions

(1) Two kinds of carbon fiber electrode were designed to investigate the electrochemical behavior on the cross-sectional (noted as OFE) and cylindrical surface (noted as UFE) of a carbon fiber, respectively.

Table 1
Estimated equivalent circuit elements of the O-CFE and U-CFE.

O-CFE, R (Ω.cm^2)	O-CFE, C (F/cm^2)	U-CFE, R_1 (Ω.cm^2)	U-CFE, R_2 (Ω.cm^2)	U-CFE, C_1 (F/cm^2)	U-CFE, C_2 (F/cm^2)
3.6×10^3	1.9×10^{-4}	1.4×10^8	3.5×10^4	2.1×10^{-7}	6.1×10^{-5}

(2) A carbon fiber is electrochemically anisotropic on different 2-dimensional surfaces. The exposed cross-sectional surface is much more active than the fiber cylindrical surface.
(3) Strong polarization damaged the carbon fiber on both the exposed cross-sectional and cylindrical surfaces. Anodic polarization was much more detrimental than cathodic polarization.
(4) A physical model for the carbon fiber electrochemical behavior was proposed. The electrochemical behavior of the cylindrical surface is like a damaged coating system. The cross-section performs just like carbon.

Declaration of competing interest

The authors have no financial or personal relationship with other researchers or organizations that may inappropriately influence the work, and there is no professional or personal interest in any product, service and/or company that could influence the position presented in, or the review of, the manuscript entitled "**Two-dimensional anisotropic electrochemical behavior of carbon fiber**".

Acknowledgement

This work was supported by GM R&D Center in Warren, Michigan, USA.

Appendix A. Supplementary data

Supplementary data to this article can be found online at https://doi.org/10.1016/j.electacta.2019.135005.

References

[1] B.A. Newcomb, Processing, structure, and properties of carbon fibers, Compos. Appl. Sci. Manuf. 91 (2016) 262–282.
[2] M. Sharma, S. Gao, E. Mäder, H. Sharma, L.Y. Wei, J. Bijwe, Carbon fiber surfaces and composite interphases, Compos. Sci. Technol. 102 (2014) 35–50.
[3] Z.P. Wen, X. Qian, Y.G. Zhang, X.F. Wang, W.X. Wang, S.L. Song, Electrochemical polymerization of carbon fibers and its effect on the interfacial properties of carbon reinforced epoxy resin composites, Compos. Appl. Sci. Manuf. 119 (2019) 21–29.
[4] J.J. Jiang, X.M. Yao, C.M. Xu, Y. Su, L.C. Zhou, C. Deng, Influence of electrochemical oxidation of carbon fiber on the mechanical properties of carbon fiber/graphene oxide/epoxy composites, Compos. Appl. Sci. Manuf. 95 (2017) 248–256.
[5] X. Huang, Fabrication and properties of carbon fibers, Materials 2 (2009) 2369–2403.
[6] Q. Yu, P. Chen, L. Wang, Degradation in mechanical and physical properties of carbon fiber/bismaleimide composite subjected to proton irradiation in a space environment, Nucl. Instrum. Methods Phys. Res. Sect. B Beam Interact. Mater. Atoms 298 (2013) 42–46.
[7] M. Lv, F. Zheng, Q. Wang, T. Wang, Y. Liang, Friction and wear behaviors of carbon and aramid fibers reinforced polyimide composites in simulated space environment, Tribol. Int. 92 (2015) 246–254.
[8] T. Heggemann, W. Homberg, Deep drawing of fiber metal laminates for automotive lightweight structures, Compos. Struct. 216 (2019) 53–57.
[9] T. Ishikawa, K. Amaoka, Y. Masubuchi, T. Yamamoto, A. Yamanaka, M. Arai, J. Takahashi, Overview of automotive structural composites technology developments in Japan, Compos. Sci. Technol. 155 (2018) 221–246.
[10] X. Qian, X. Wang, Q. Ouyang, Y. Chen, Q. Yan, Effect of ammonium-salt solutions on the surface properties of carbon fibers in electrochemical anodic oxidation, Appl. Surf. Sci. 259 (2012) 238–244.
[11] C. Wang, X. Ji, A. Roy, V.V. Silberschmidt, Z. Chen, Shear strength and fracture toughness of carbon fibre/epoxy interface: effect of surface treatment, Mater. Des. 85 (2015) 800–807.
[12] S. Tiwari, J. Bijwe, S. Panier, Optimization of surface treatment to enhance fiber-matrix interface and performance of composites, Wear 274 (2012) 326–334.
[13] F. Severini, L. Formaro, M. Pegoraro, L. Posca, Chemical modification of carbon fiber surfaces, Carbon 40 (2002) 735–741.
[14] L. Meng, D. Fan, C. Zhang, Z. Jiang, Y. Huang, The effect of oxidation treatment by KClO3/H2SO4 system on intersurface performance of carbon fibers, Appl. Surf. Sci. 268 (2013) 225–230.
[15] H. Guo, Y.D. Huang, L.H. Meng, L. Liu, D.P. Fan, D.X. Liu, Interface property of carbon fibers/epoxy resin composite improved by hydrogen peroxide in supercritical water, Mater. Lett. 63 (2009) 1531–1534.
[16] J. Liu, Y. Tian, Y. Chen, J. Liang, L. Zhang, H. Fong, A surface treatment technique of electrochemical oxidation to simultaneously improve the interfacial bonding strength and the tensile strength of PAN-based carbon fibers, Mater. Chem. Phys. 122 (2010) 548–555.
[17] X. Qian, J.H. Zhi, L.Q. Chen, J. Huang, Y.G. Zhang, Effect of low current density electrochemical oxidation on the properties of carbon fiber-reinforced epoxy resin composites, Surf. Interface Anal. 45 (2013) 937–942.
[18] D.K. Kim, K.H. An, Y.H. Bang, L.K. Kwac, S.Y. Oh, B.J. Kim, Effects of electrochemical oxidation of carbon fibers on interfacial shear strength using a micro-bond method, Carbon Letters 19 (2016) 32–39.
[19] M. Andideh, M. Esfandeh, Statistical optimization of treatment conditions for the electrochemical oxidation of PAN-based carbon fiber by response surface methodology: application to carbon fiber/epoxy composite, Compos. Sci. Technol. 134 (2016) 132–143.
[20] Z.T. Lin, B. Zhu, X. Lin, Y. Chen, Y.Z. Liu, Study on surface properties of PAN-based carbon fiber oxidized in a static electrochemical oxidation process, Adv. Mater. Res. 774–776 (2013) 1103–1106.
[21] S. Tiwari, M. Sharma, S. Panier, B. Mutel, P. Mitschang, J. Bijwe, Influence of cold remote nitrogen oxygen plasma treatment on carbon fabric and its composites with specialty polymers, J. Mater. Sci. 46 (2011) 964–974.
[22] C.U. Pittman, W. Jiang, G.R. He, S.D. Gardner, Oxygen plasma and isobutylene plasma treatments of carbon fibers: determination of surface functionality and effects on composite properties, Carbon 36 (1998) 25–37.
[23] Z. Wang, X.Y. Huang, G.J. Xian, H. Li, Effects of surface treatment of carbon fiber: tensile property, surface characteristics, and bonding to epoxy, Polym. Compos. 37 (2016) 2921–2932.
[24] C.U. Pittman, W. Jiang, Z.R. Yue, S. Gardner, L. Wang, H. Toghiani, C. Leon, Surface properties of electrochemically oxidized carbon fibers, Carbon 37 (1999) 1797–1807.
[25] H. Yuan, C. Wang, S. Zhang, X. Lin, Effect of surface modification on carbon fiber and its reinforced phenolic matrix composite, Appl. Surf. Sci. 259 (2012) 288–293.
[26] Y.Y. Zhang, Y.Z. Zhang, Y. Liu, X.L. Wang, B. Yang, A novel surface modification of carbon fiber for high-performance thermoplastic polyurethane composites, Appl. Surf. Sci. 382 (2016) 144–154.
[27] J.J. Jiang, X.M. Yao, C.M. Xu, Y. Su, C. Deng, F. Liu, J.J. Wu, Preparation of graphene oxide coatings onto carbon fibers by electrophoretic deposition for enhancing interfacial strength in carbon fiber composites, J. Electrochem. Soc. 163 (2016) D133–D139.
[28] D.D.L. Chung, Chapter 3 - structure of carbon fibers, in: D.D.L. Chung (Ed.), Carbon Fiber Composites, Butterworth-Heinemann, Boston, 1994, pp. 55–64.
[29] C. Zhang, D. Zheng, G.L. Song, Y. Guo, M. Liu, H. Kia, Effect of the microstructure of carbon fiber reinforced polymer on electrochemical behavior, J. Electrochem. Soc. 165 (2018) C647–C656.
[30] M. Tavakkolizadeh, H. Saadatmanesh, Galvanic Corrosion of Carbon and Steel in Aggressive Environments, vol. 5, American Society of Civil Engineers, 2014, pp. 200–210.
[31] G.J. Brug, A.L.G. van den Eeden, M. Sluyters-Rehbach, J.H. Sluyters, The analysis of electrode impedances complicated by the presence of a constant phase element, J. Electroanal. Chem. Interfacial Electrochem. 176 (1984) 275–295.
[32] P. Sharma, T.S. Bhatti, A review on electrochemical double-layer capacitors, Energy Convers. Manag. 51 (2010) 2901–2912.
[33] H. Shi, Activated carbons and double layer capacitance, Electrochim. Acta 41 (1996) 1633–1639.
[34] T. Pajkossy, D.M. Kolb, Double layer capacitance of Pt(111) single crystal electrodes, Electrochim. Acta 46 (2001) 3063–3071.
[35] X. Liu, J. Xiong, Y. Lv, Y. Zuo, Study on corrosion electrochemical behavior of several different coating systems by EIS, Prog. Org. Coat. 64 (2009) 497–503.
[36] J. Ryou, S. Shah, Detecting corrosion resistance of coated steel rebars by electrochemical technique (EIS), Surf. Rev. Lett. 13 (2006) 345–349.
[37] S. Chen, H. Hou, F. Harnisch, S.A. Patil, A.A. Carmonamartinez, S. Agarwal, Y. Zhang, S. Sinharay, A.L. Yarin, A. Greiner, Electrospun and solution blown three-dimensional carbon fiber nonwovens for application as electrodes in microbial fuel cells, Energy Environ. Sci. 4 (2011) 1417–1421.
[38] J. Ledesma-García, I.L.E. García, F.J. Rodríguez, T.W. Chapman, L.A. Godínez, Immobilization of dendrimer-encapsulated platinum nanoparticles on pretreated carbon-fiber surfaces and their application for oxygen reduction, J. Appl. Electrochem. 38 (2008) 515–522.
[39] Y. Luo, H. Yang, J. Luo, C.M. Li, J. Jiang, W. Zhou, X. Qi, H. Zhang, D.Y.W. Yu, T. Yu, Self-assembly of well-ordered whisker-like manganese oxide arrays on carbon fiber paper and its application as electrode material for supercapacitors, J. Mater. Chem. 22 (2012) 8634–8640.
[40] J.K. Kim, C.S. Park, D.W. Lee, S.M. Cho, C.R. Han, Measurement of the gauge factor of carbon fiber and its application to sensors, Microelectron. Eng. 85 (2008) 787–791.
[41] Y. Chiun-Jye, W. Chung-Liang, W. Teng Yang, H. Kuo-Chu, C. Wei-Chi, Fabrication of a carbon fiber paper as the electrode and its application toward developing a sensitive unmediated amperometric biosensor, Biosens. Bioelectron. 26 (2011) 2858–2863.
[42] C. Zhang, D.J. Zheng, G.-L. Song, Y. Guo, M. Liu, H. Kia, Corrosion behavior of the joints of carbon fiber reinforced polymers with DP590 steel and Al6022 alloy, Anti-Corrosion Methods & Mater. 66 (2019) 479–485.